

Optimal cytoplasmatic density and flux balance model under macromolecular crowding effects

Alexei Vazquez

Department of Radiation Oncology, The Cancer Institute of New Jersey and UMDNJ-Robert Wood Johnson Medical School
195 Little Albany St, New Brunswick, NJ 08903, USA

(Dated: November 21, 2018)

Macromolecules occupy between 34 and 44% of the cell cytoplasm, about half the maximum packing density of spheres in three dimension. Yet, there is no clear understanding of what is special about this value. To address this fundamental question we investigate the effect of macromolecular crowding on cell metabolism. We develop a cell scale flux balance model capturing the main features of cell metabolism at different nutrient uptakes and macromolecular densities. Using this model we show there are two metabolic regimes at low and high nutrient uptakes. The latter regime is characterized by an optimal cytoplasmatic density where the increase of reaction rates by confinement and the decrease by diffusion slow-down balance. More important, the predicted optimal density is in the range of the experimentally determined density of *E. coli*. We conclude that cells have evolved to a cytoplasmatic density resulting in the maximum metabolic rate given the nutrient availability and macromolecular crowding effects and report a flux balance model accounting for its effect.

Macromolecular crowding affects the rate of biochemical reactions [1]. It tends to increase reaction rates by increasing enzyme concentrations and to decrease reaction rates by reducing the diffusion coefficient of metabolites. The competition between these two factors results in a maximum reaction rate at intermediate crowding agent concentrations [1]. Yet, it remains to be addressed whether this observation is true at the level of the whole cell metabolism. The macromolecular volume fraction of the *E. coli* cytoplasm is in the range 0.34-0.44 [2], half the maximum packing density of spheres in three dimension. This observation indicates cell metabolism is operating under the crowding conditions created by its macromolecular components.

To investigate the effect of macromolecular crowding in the overall cell metabolism we focus on the model schematically represented in Fig. 1. (i) From the perspective of cell metabolism alone the cytoplasm is composed of metabolites and enzymes, the latter including metabolic enzymes, ribosomes and any other macromolecule catalyzing metabolic/biosynthetic processes. (ii) Metabolites are relatively small compared to enzymes and we neglect their contribution to crowding. (iii) The active site of most metabolic enzymes is relatively small compared to the whole enzyme. For all practical purposes the inert enzyme region is equivalent to an inert crowding agent. The inert region reduces the volume available to all solutes and, from a point of view of diffusion, collisions between metabolites and the inert region of enzymes are equivalent to collisions between the metabolites and inert crowding agents. Therefore, we model the contribution of active sites and the inert mass independently. We assume that each enzyme molecule contributes as two different fictitious quasi-molecules: one representing the enzyme active site (or union of active sites) and the other the inert enzyme region (Fig. 1b). The active site quasi-molecule is assumed

to occupy a relatively small volume and its contribution to crowding is neglected. Its diffusion coefficient is assumed to be, however, the same as that for the original enzyme. The quasi-molecule representing the inert enzyme region is modeled as an inert crowding agent, with a size and diffusion coefficient equal to that of the corresponding enzyme. Because of their relatively larger sizes, enzymes have smaller diffusion coefficients than metabolites. We thus approximate the relative diffusion coefficient between enzymes and metabolites by the diffusion coefficient of the metabolites.

(iv) In a crowded media concentrations are effectively higher because part of the volume is occupied by the crowding agents. The ratio between the effective concentration C and the concentration in an ideal solution C_0 is denoted by the activity coefficient $\gamma_C = C/C_0$. When the solute interacts with the crowding agents exclusively via steric repulsion $\gamma_C = V/V_a$ [3], where V is the total volume and V_a is the volume available to the solute. The volume available to a solute can be approximated by the total volume minus the volume occupied by all crowding agents, resulting in

$$\gamma_C = \frac{1}{1-v}, \quad (1)$$

where v is the macromolecular volume fraction.

(v) The diffusion coefficient of a trace particle in a crowding media is also affected by the concentration of crowding agents. In general the diffusion coefficient is given by $D = \gamma_D D_0$, where D_0 is the diffusion coefficient in aqueous solution and γ_D is a correction factor. To quantify the impact of crowding on metabolites diffusion we use the empirical exponential law

$$\gamma_D = e^{-\alpha v}, \quad (2)$$

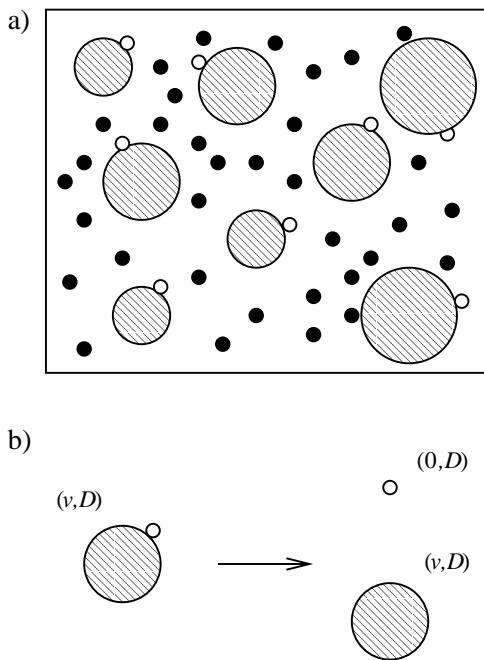


FIG. 1: **Metabolic model of the cytoplasm.** a) Schematic representation of the cytoplasm from the perspective of cell metabolism. The solid circles represent small metabolites. The dashed circles with attached small empty circles represent metabolic enzymes, the former representing their inert region and the latter the active site. b) We model an enzyme of molecular volume v and diffusion coefficient D as two different quasi-molecules. One representing the active site, with zero (or negligible) molecular volume and the same diffusion coefficient. The other representing the enzyme inert region, with same molecular volume and diffusion coefficient as the whole enzyme.

where the exponent α is an empirical parameter [4, 5, 6, 7]. The closest estimate for the cytoplasm comes from the experimental report $\alpha = 5.8$ for fibroblast cells [5].

(vi) The kinetic models describing the rate of biochemical reactions as a function of the concentration of reacting metabolites can be quite complex and are unknown for most metabolic reactions. For example, consider the simple case where a substrate S is irreversibly transformed into the product P catalyzed by the enzyme E , with concentrations S , P , and E , respectively. The rate of this reaction is given by the Michaelis-Menten model $R = k_2SE/(K_M + S)$, where k_2 is the rate of the conversion of the intermediate enzyme-substrate complex ES into the product $ES \rightarrow P$, $K_M = (k_{-1} + k_2)/k_1$ is the Michaelis-Menten or half-saturation constant, and k_{-1} and k_1 are the rate of the intermediate steps $ES \rightarrow E + S$ and $E + S \rightarrow ES$, respectively. The step $E + S \rightarrow ES$ is diffusion limited and $k_1 = 4\pi Da$, where D is the substrate diffusion coefficient and a is the effective size of the enzyme active site. *Diffusion limited regime:* When $S \ll K_M$ the reaction rate can be approximated by $R \approx [k_2/(k_{-1} + k_2)]k_1SE \propto DE$ and therefore the over-

all reaction is diffusion limited. In this limit most active sites are free and the reaction rate is limited by the rate of encounter of the enzyme active site and the substrate. *Saturation regime:* When $S \gg K_M$ the reaction rate is approximated by $R \approx k_2E$. In this case most active sites are occupied and the reaction rate is limited by the chemical step $ES \rightarrow P$. The situation becomes more complicated for reactions involving more than one substrate, because of reversibility and other factors. Nevertheless, in general these two limiting scenarios, diffusion limited and saturation persist. As a first approximation we therefore assume that biochemical reactions are divided into two groups: a set \mathcal{L} of diffusion limited reactions and a set \mathcal{S} of reactions at saturation, with reaction rates given by

$$R_i = \begin{cases} g_i D_i C_i, & \text{for } i \in \mathcal{L} \\ k_i C_i & \text{for } i \in \mathcal{S} \end{cases} \quad (3)$$

where g_i is a model parameter containing all other contributions in the diffusion limited regime (e.g. metabolite concentrations) and k_i is the rate of reaction i in the saturation limit.

(vi) At the level of cell metabolism we use a steady state or flux balance model [8]. In the steady state the consumption and production of each metabolite balance

$$\sum_i S_{ji} R_i = 0, \quad (4)$$

where $i = 1, \dots, n$ as above is an index over reactions, $j = 1, \dots, m$ is an index over the metabolites, and S_{ji} is the stoichiometric coefficient of metabolite j in reaction i [8]. To account for the potential existence of a limiting nutrient we label by $i = 1$ a reaction representing the nutrient uptake and assume

$$R_1 \leq U, \quad (5)$$

where U denotes the maximum uptake of the limiting nutrient. We also label by $i = n$ the metabolic objective or biomass vector, an effective reaction with a nonzero stoichiometric coefficient for each metabolite the cell produces and magnitude given by its relative ratio. Thus R_n is our measure of metabolic rate.

(vii) Given a flux distribution R_i we now calculate the volume fraction occupied by enzymes. The metabolic enzymes are characterized by their concentration C_{0i} , occupied volume fraction v_i , molar mass μ_i , specific volume ν_i and kinetic model (3). The occupied volume fraction is related to the enzyme concentration through the equation $v_i = \mu_i \nu_i C_{0i}$. In turn the enzyme concentration is related to the reaction rate through (3). Putting these two relationships together, recalling that $C_i = \gamma_C C_{0i}$ and $D_i = \gamma_D D_{0i}$, and using (1) and (2), we obtain

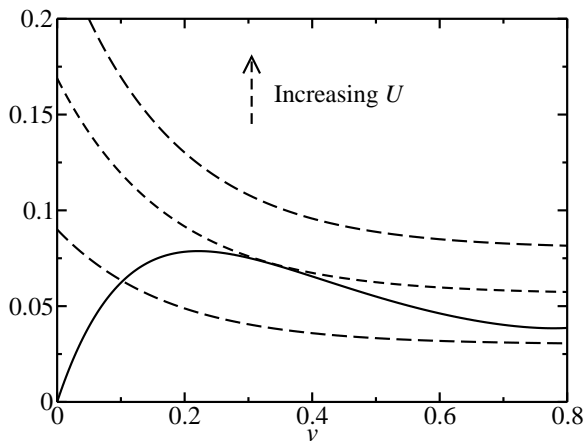


FIG. 2: **Calculation of the optimal volume fraction.** The left (solid line) and right (dashed lines) hand side of (7) for different values of U , assuming $S/L = 2$ and $UL = 0.03, 0.057$ and 0.08 from bottom to top. The intersection between these lines determines the optimal volume fraction v^* . For the upper dashed line, representing a larger U , there is no solution.

$$v_i = (1 - v)R_i \times \begin{cases} \frac{\mu_i \nu_i}{g_i D_{0i}} e^{\alpha v}, & \text{for } i \in \mathcal{L} \\ \frac{\mu_i \nu_i}{k_i}, & \text{for } i \in \mathcal{S}. \end{cases} \quad (6)$$

At this point we add up the volume fraction occupied by enzymes $v = \sum_i v_i$, which after some algebra results in

$$\frac{v e^{-\alpha v}}{1 - v} = U [L(r) + S(r) e^{-\alpha v}], \quad (7)$$

$$L(r) = \sum_{i \in \mathcal{L}} \frac{\mu_i \nu_i}{g_i D_{0i}} r_i, \quad S(r) = \sum_{i \in \mathcal{S}} \frac{\mu_i \nu_i}{k_i} r_i. \quad (8)$$

where $r_i = R_i/U$ are the reaction rates in units of U .

Under the model (i)-(vii), the optimal reaction rates R_i , $i = 1, \dots, n$, and volume fraction v are obtained maximizing the metabolic objective R_n , subject to the flux balance (4), uptake capacity (5) and solvent capacity (7)-(8) constraint. The solution of this optimization problem results in the following regimes.

Nutrient limited: There is a threshold uptake capacity U_c such that for $U < U_c$ the optimal reaction rates, denoted by $r_i^{(1)}$, are those maximizing the metabolic objective R_n subject to the flux balance (4) and uptake capacity (5) constraint, $r_i^{(1)}$ are independent of U , and there is a volume fraction v satisfying (7) with $L = L(r^{(1)})$ and $S = S(r^{(1)})$. The existence of this threshold uptake capacity is derived from the analysis of solutions to (7) with respect to v , given L and S (Fig. 2). The left hand side has a maximum at

$$v_0 = \begin{cases} v_m, & 0 < \alpha < 4 \\ \frac{1}{2} \left(1 - \sqrt{1 - \frac{4}{\alpha}} \right), & \alpha \geq 4. \end{cases} \quad (9)$$

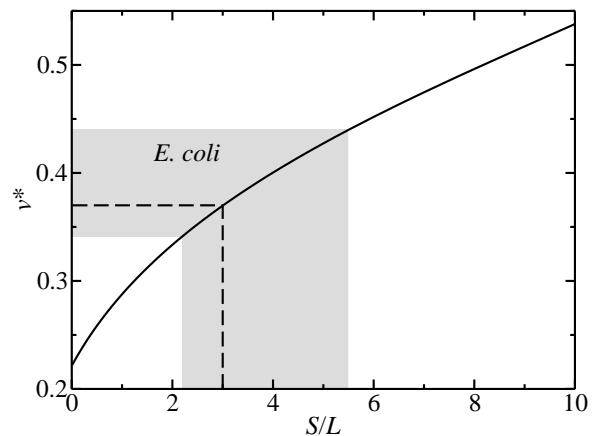


FIG. 3: **Optimal volume fraction.** The optimal volume fraction for $\alpha = 5.8$ as a function of the ratio S/L (solid line). The shadowed area was obtained using as input the volume fraction range 0.34 - 0.44 for *E. coli* [2] and computing the associated S/L range from (7). The dashed line represents our prediction $v^* = 0.37$ assuming $S/L = 3$.

On the other hand the right hand side is a decreasing function of v , starting from $U(L + S)$ at $v = 0$ and ending at $U(L + S e^{-v_m})$ at $v = v_m$, where v_m denotes the maximum packing density of the cytoplasmatic components. For small values of U the two curves intercept and (7) has a solution $v = v(U, S/L)$, which is an increasing function of U . There is no solution, however, for large values of U . The maximum values of U and v where a solution exists, denoted by U_c and v^* , are obtained when the tangents of the left and right hand side of (7) are equal as well. The simultaneous solution of these two equations results in an explicit relation between U_c and v^* , and a transcendental equation for v^* parametrized by α and S/L . For the intracellular value $\alpha = 5.8$ we compute the maximum cell density as a function of S/L (Fig. 3). It increases monotonically starting from $v_0 \approx 0.22$ (9) when all reactions are diffusion limited.

Space limited: For $U > U_c$ we cannot further increase the volume fraction beyond v^* and (7) becomes a constraint on the reaction rates. In this regime the optimal reaction rates are obtained maximizing the metabolic objective R_n subject to the flux balance (4), the uptake capacity (5), and the solvent capacity constraint

$$\sum_i a_i R_i = 1, \quad (10)$$

$$a_i = \begin{cases} \frac{\mu_i \nu_i}{g_i D_{0i}} \frac{1 - v^*}{v^*} e^{\alpha v^*}, & \text{for } i \in \mathcal{L} \\ \frac{\mu_i \nu_i}{k_i} \frac{1 - v^*}{v^*}, & \text{for } i \in \mathcal{S}. \end{cases} \quad (11)$$

An equation similar to (10) has been introduced before under the name of macromolecular crowding or solvent capacity constraint [9]. The coefficients a_i have been

named crowding coefficients as they quantify how much the reactions contribute to the crowding of the cytoplasm. Equation (11) now introduces corrections to the previous calculations [9], making a more precise accounting for the effect of macromolecular crowding on reactions rates.

To provide a quantitative prediction for the optimal volume fraction we need an estimate of S/L . Given that the kinetic parameters involved in these calculations are unknown for most biochemical reactions we cannot make a precise calculation at this point. Recent metabolite concentration measurements for *E. coli* [10] indicate that 83% of the reactions have $S > K_M$, i.e. there are about three times more reactions in the saturation regime. Assuming that the values of $g_i D_{0i}$ and k_i are not significantly different we would conclude that S is about three times larger than L . In this case our calculations predict an optimal volume fraction of 0.37 (see Fig. 3). Experimental estimates of the macromolecular volume fraction of the *E. coli* cytoplasm indicate the lower and upper bounds 0.34 and 0.44 respectively [2], containing the crude estimate 0.37 predicted above. A more conservative prediction is the interval between the lower bound 0.22 when all reactions are diffusion limited and the upper bound given by the maximum packing density v_m when all reactions are at saturation. The latter can reach values as high as 0.8 when the particles have variable size [11]. This conservative range also contains the experimental report between 0.34 and 0.44 for *E. coli* [2].

In summary, there are two different metabolic regimes, nutrient limited and nutrient limited with a solvent capacity constraint. In the nutrient limited regime the metabolic rate is constrained by the stoichiometry of the set of biochemical reactions and the maximum uptake rate of the limited nutrient. In the nutrient limited with a solvent capacity constraint the metabolic rate is in addition constrained by macromolecular crowding effects. In particular there is an optimal macromolecular volume fraction resulting in the maximum metabolic objective. The optimal volume fraction is a function of the diffusion related exponent α and the ratio of reactions in a diffusion limited and saturation regimes. It interpolates between $v^* \approx 0.22$ when all reactions are diffusion limited and the maximum packing density when all reactions are at saturation. Finally, we can write a general flux balance model that applies for both regimes: maximize the metabolic objective R_n subject to the flux balance $\sum_i S_{ji} R_i = 0$, uptake capacity $R_i \leq U$ and solvent capacity $\sum_i a_i R_i \leq 1$ constraint. The latter inequality is satisfied with the less than sign for $U < U_c$ and with the equal sign for $U > U_c$.

We have made several assumptions that could affect the obtained results. The equations (1) and (2) characterizing the impact of macromolecular crowding on effective enzyme concentrations and metabolite diffusion

coefficients may require further corrections when the occupied volume fraction gets closer to the maximum packing density. In the intracellular media the typical occupied volume fraction is about half the maximum packing density 0.74 of spheres in three dimensions. Therefore, we expect equations (1) and (2) to be sufficiently good approximations. The kinetic models cannot always be approximated by the extreme cases of diffusion limited and saturation regimes. As a consequence the plot in Fig. 3 may be slightly different.

Taking together our results indicate that at high metabolic rates there is an optimal intracellular density where the increase of reaction rates by confinement and the decrease by diffusion slow-down balance. Since it is the optimal density resulting in the maximum metabolic rate, an increase of the density of enzymes beyond this optimal value will result in a decrease of the metabolic rate. Although this may sound counter intuitive, it follows from the fact that beyond the optimal density the slow-down of diffusion starts to dominate, diminishing the overall metabolic rate. More important, the experimentally determined density of *E. coli* is in the range predicted from our model. We thus claim that cells have evolved an intracellular density that results in maximum metabolic capabilities given the macromolecular crowding effects.

Acknowledgements: Many thanks to The Simons Center for Systems Biology at the Institute for Advanced Study where part of this work was performed.

-
- [1] A. P. Minton, J. Biol. Chem. **276**, 10577 (2001).
 - [2] S. B. Zimmerman and S. O. Trach, J. Mol. Biol. **222**, 599 (1991).
 - [3] J. L. Lebowitz, E. Helfand, and E. Praestgaard, J. Chem. Phys. **43**, 774 (1965).
 - [4] R. Furukawa, J. L. Arauz-Lara, and B. R. Ware, Macromolecules **24**, 599 (1991).
 - [5] H. P. Kao, J. R. Abney, and A. S. Verkman, J. Cell Biol. **120**, 175 (1993).
 - [6] E. Dauty and A. S. Verkman, J. Mol. Recognit **17**, 441 (2004).
 - [7] J. A. Dix and A. S. Verkman, Ann. Rev. Biophys. **37**, 247 (2008).
 - [8] J. S. Edwards, M. Covert, and B. O. Palsson, Environ. Microbiol. **4**, 133 (2002).
 - [9] A. Vazquez, Q. K. Beg, M. A. de Menezes, Z. B.-J. Ernst, A.-L. Barabasi, L. G. Boros, and Z. N. Oltvai, BMC Syst. Biol. **2**, 7 (2008).
 - [10] B. D. Bennett, E. H. Kimball, M. GAo, R. Osterhout, S. J. V. Dien, and J. D. Rabinowitz, Nat. Rev. Chem. Biol. **5**, 593 (2009).
 - [11] H. Y. Sohn and C. Moerland, Canadian J Chem Engin **46**, 162 (1968).